

1
2
3
4
5
6
7
8
9

Observation of flux tube crossings in the solar wind

L. Arnold¹, G. Li^{1,*}, X. Li¹, Y. Yan²

¹ Department of Physics and CSPAR, University of Alabama in Huntsville 35899, USA,
gang.li@uah.edu

² Key Laboratory of Solar Activity, National Astronomical Observatories of Chinese
Academy of Sciences, Beijing 100012, China

Published: The Astrophysical Journal, 766, 2, 2013,

doi:10.1088/0004-637X/766/1/2

10 **ABSTRACT**

11 Current sheets are ubiquitous in the solar wind. They are a major source of the solar wind MHD turbulence intermittency. They may result from non-linear interactions of the solar wind MHD turbulence or are the boundaries of flux tubes that originate from the solar surface. Some current sheets appear in pairs and are the boundaries of transient structures such as magnetic holes and reconnection exhausts, or the edges of pulsed Alfvén waves. For an individual current sheet, discerning whether it is a flux tube boundary or due to non-linear interactions, or the boundary of a transient structure is difficult. In this work, using data from the *Wind* spacecraft, we identify two three-current-sheet events. Detailed examination of these two events suggest that they are best explained by the flux tube crossing scenario. Our study provides a convincing evidence supporting the scenario that the solar wind consists of flux tubes where distinct plasmas reside.

12 **1. Introduction**

13 The solar wind provides a natural environment to study MHD turbulence in a
14 collisionless plasma. Over the past few decades the launches of spacecraft such as Voyager,
15 Helios, Ulysses, *Wind*, and ACE have made available a significant amount of data for
16 analyzing the solar wind MHD turbulence.

17 The first theory of hydrodynamic turbulence, suggested by Kolmogorov (1941),
18 known as the K41 theory, predicted a magnetic field power-law spectrum $\sim k^{-5/3}$. This
19 $-5/3$ exponent arises from the nonlinear interactions of the homogeneous hydrodynamic
20 turbulence in which energy is cascaded from large scales to small scales. For incompressible
21 MHD turbulence where the cascading process is mediated by counter-propagating Alfvén

22 wave packets, the Iroshnikov-Kraichnan (IK) theory (Iroshnikov 1964; Kraichnan 1965) and
23 some recent theories of strong MHD turbulence (Boldyrev 2006; Boldyrev and Perez 2009)
24 predict a power spectrum $\sim k^{-3/2}$.

25 One important concept in turbulence is intermittency. Ruzmaikin et al. (1995)
26 suggested that intermittent structures can affect the solar wind MHD turbulence power
27 spectrum. They pointed out that the effect of intermittency in the solar wind MHD
28 turbulence is to reduce the exponent of the power law spectrum. Ruzmaikin et al. (1995)
29 further suggested that intermittency is “in the form of ropes, sheets or more complicated
30 fractal forms.” Recently, in studying current sheets (CS) in the solar wind, Li et al. (2011)
31 found that the power spectrum of solar wind magnetic field behaves as K41 in periods that
32 have abundant numbers of current sheets and behaves as IK in periods that are almost
33 current-sheet free (see also Borovsky (2010)). Since these current sheets are a source of
34 intermittency, the study of Li et al. (2011) supports Ruzmaikin et al. (1995).

35 A current sheet is a 2D structure across which the magnetic field direction changes
36 abruptly. Current sheets can be of large scales. For example, the heliospheric current sheet
37 and current sheets found in CME-driven shocks are all large scale current sheets. These are
38 not the subjects of this study. Here we consider current sheets that are of small scales.

39 Some current sheets occur in pairs. These can be tangential discontinuities (TDs),
40 often forming the two boundaries of a magnetic hole (see the review of Tsurutani et al.
41 (2011) and references therein), or rotational discontinuities (RDs) which are the boundaries
42 of an exhaust from a reconnection site (see (Gosling et al. 2005) and the review of Gosling
43 (2011)). Comparing to magnetic holes, reconnection exhausts can be of larger scales.
44 Gosling (2007) has found that the typical width of a reconnection exhaust is $\sim 10^4$ km and
45 some reconnection exhausts can be as wide as 10^5 km. Consequently, these boundaries may
46 be practically identified as “single-current-sheet” event.

47 Most current sheets do not occur in pairs. These current sheets can be generated
48 through non-linear interactions in the MHD turbulence (Zhou et al. 2004; Chang et al.
49 2004). Using ACE data, Vasquez et al. (2007) examined magnetic field discontinuities
50 which can have very small spread angles for Bartels rotation 2286 (day 7 to 33 in 2001).
51 They found that the statistical properties of these discontinuities form a single population
52 and they are consistent with turbulence generated in-situ. By examining the probability
53 density functions (PDF) of the magnetic field components from a 1D spectral code,
54 Greco et al. (2008) showed that current sheets often occur at the super Gaussian tail of the
55 PDF. Moreover, Greco et al. (2009) found that, at the inertial scale, in which the energy
56 cascading rate is independent of the scale, the PDF of waiting times (WTs) between MHD
57 discontinuities that are identified in the solar wind using the method of Tsurutani & Smith
58 (1979) and those from MHD simulations are very similar, suggesting that these structures
59 can be explained as a natural result of the non-linear interaction of the solar wind MHD
60 turbulence.

61 Other opinions exist. In an earlier work, Bruno et al. (2001) studied current sheets in
62 the solar wind by analyzing Helios 2 data using the minimum variance method to show how
63 the magnetic field changed over selected time periods. Bruno et al. (2001) were the first
64 to suggest that these structures may be boundaries between flux tubes. Borovsky (2008)
65 analyzed an extended time period of magnetic field from the ACE spacecraft and examined
66 the distribution of the spread angle across the current sheets. He showed that the angle
67 distribution has two populations and suggested that the second population, dominating at
68 large angles, could be “magnetic walls” and originate from the surface of the Sun. A solar
69 wind that consists of many flux tubes can be viewed as a structured solar wind. In both
70 the work of Bruno et al. (2001) and Borovsky (2008), the solar wind is envisioned to be full
71 of structures, the flux tubes. Observed at a spacecraft, these structures are convected out
72 with the solar wind. A similar scenario where structures convecting out from the Sun has

73 been proposed by Tu and Marsch (1991). Analysis on the cross helicity σ_c and residual
74 energy σ_r by Bruno et al. (2007) supported the proposal of Tu and Marsch (1991).

75 Regardless the origin of a current sheet, Li (2008) developed a procedure to
76 systematically identify these structures. Using this procedure, Li et al. (2008) examined
77 current sheets in the solar wind and in the Earth’s magnetotail using *Cluster* magnetic
78 field data and concluded that current sheets are more abundant in the solar wind. Later,
79 Miao et al. (2011) examined over 3 years’ worth slow wind data using *Ulysses* observations
80 and found there were 2 populations for the distribution of the spread angle across current
81 sheets, in agreement with Borovsky (2008).

82 Perhaps a large fraction of current sheets identified in the solar wind are due to
83 the non-linear interactions of the solar wind MHD turbulence, as shown in the work of
84 Greco et al. (2008, 2009). However, a statistical study such as Greco et al. (2008, 2009)
85 can not rule out the possibility that some current sheets in the solar wind are boundaries
86 of flux tubes. Indeed, Borovsky (2008) has used plasma data including proton density
87 and temperature, Helium abundance, electron strahl strength, etc. to identify possible
88 plasma boundaries. Plasma data, however, is often of lower time resolution than magnetic
89 field data. Furthermore, plasmas in different flux tubes may have similar properties except
90 different velocities and magnetic field directions. Therefore, to unambiguously separate
91 these two populations can be hard. Note, the occurrence rates of these two populations
92 may have different radial dependence and/or different solar wind type dependence.

93 In this work, as an effort to identify flux tubes in the solar wind, we present a case study
94 of two “triple-current-sheet” event using data from spacecraft *Wind*. A triple-current-sheet
95 event is where three current sheets occurred in a relatively short period of time. The reason
96 that we want to search for a triple-current-sheet event is the following. In the flux-tube
97 scenario, the solar wind plasmas reside in different flux tubes and the solar wind magnetic

98 field and plasma properties differ in these flux tubes. Since flux tubes are 3D structures, we
99 expect the boundary between two adjacent flux tubes to be curved and have small-scale
100 ripples. This is shown in the cartoons in Figure 1. As these flux tubes are convected out
101 past a spacecraft, depending on the relative configuration of the spacecraft trajectory and
102 these ripples, one expects to observe most often a single crossing as in Figure 1 (a), and
103 sometimes a double crossing as in Figure 1 (b), and occasionally a triple crossing as in
104 Figure 1 (c). These three different cases are referred to as “single-current-sheet” events,
105 “double-current-sheet” events, and “triple-current-sheet” events in this study.

106 A triple-current-sheet event can be used to discriminate between the scenario where
107 current sheets are generated in-situ and the scenario where current sheets originate from the
108 surface of the Sun. In the former case, one expects no correlations between these current
109 sheets in the sense that plasmas before and after these current sheet crossings need not
110 show any relationships. In the latter case, however, the spacecraft traverses through two
111 distinct plasmas in the sequence of “I, II, I, II”, so the observed plasma properties do not
112 vary arbitrarily.

113 2. Data Selection and Analysis

114 We use the 3 s plasma and magnetic field data from the 3DP (Lin et al. (1995)) and
115 magnetic field (Lepping et al. (1995)) experiments on the *Wind* spacecraft. The data
116 period was from September to October of 1995, which was during the declining phase of the
117 solar cycle. It is ideal to select data in the solar minimum period due to lack of transient
118 structures such as CMEs. For the data analysis method of current sheet identification, the
119 readers are referred to Li (2008) and Miao et al. (2011).

120 In the following, we first present a single-current-sheet event and a double-current-sheet

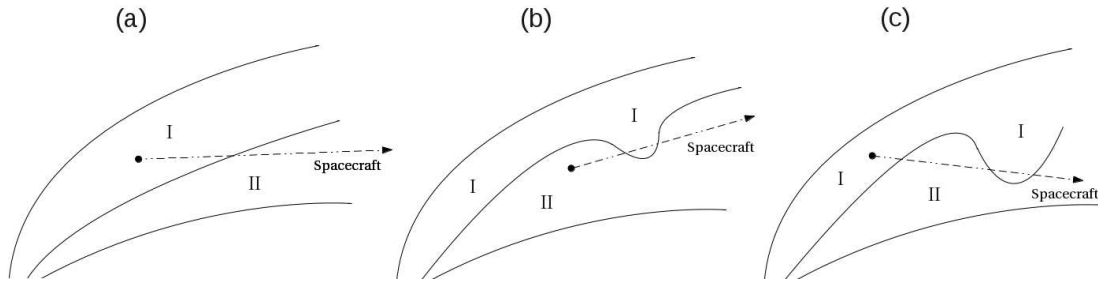


Fig. 1.— Cartoons illustrating (a) a single-current-sheet event, (b) a double-current-sheet event, and (c) a triple-current-sheet event. Note that in the case of triple-current-sheet event, the spacecraft traverses through two distinct plasmas in the sequence of “I, II, I, II”. Consequently, we expect to find the plasma properties to vary accordingly. Dashed line with arrow represents the relative trajectory of the *Wind* spacecraft passing through the flux tubes.

121 event. We then present two triple-current-sheet events.

122 Figure 2 is a single-current-sheet event which occurred on 1995-09-21. The current
 123 sheet in Figure 2 is located at 14:32 UT and is shown by the brown vertical line. Before
 124 the current sheet the magnetic field magnitude $|B|$ decreases and the proton density
 125 N_p increases. In the scenario where a current sheet is the boundary of a flux tube,
 126 these changes across the current sheet occur because plasmas in different flux tubes have
 127 different properties (as shown in panel (a) of Figure 1). However, one need not invoke the
 128 flux-tube-crossing scenario to explain Figure 2. It can be simply a tangential discontinuity
 129 (TD) or one side of a reconnection exhaust. Indeed, careful examination shows that there
 130 was another small current sheet on $\sim 14 : 32$ UT, when $|B|$ decreased and N_p increased.
 131 Our selection procedure did not pick out this earlier current sheet.

132 The change across the current sheets are Alfvénic. The angle between $\delta\vec{B}$ and $\delta\vec{V}$ across
 133 the current sheet is 7° . For the earlier current sheet (that did not get picked up by our
 134 procedure), the angle is 173° . Such parallel and anti-parallel Alfvénic changes are always

135 associated with a reconnection exhaust (Gosling 2011). Furthermore, there was also a
136 decrease of magnetic field and an increase of number density (but not temperature) between
137 these two current sheets, providing another support for identification of a reconnection
138 exhaust. Therefore, Figure 2, although identified as a single-current-sheet event using the
139 Li (2008) algorithm, is really part of a pair of a bifurcated current sheet (Gosling et al.
140 2005; Gosling 2007, 2011).

141 Figure 3 is a double-current-sheet event. Two current sheets can be identified around
142 11:11:48 UT and 11:12:26 UT. In the scenario of flux-tube-crossing, Figure 3 can be
143 understood as the spacecraft briefly crosses the magnetic wall between two flux tubes and
144 then returns to the original flux tube. The schematic of this event is shown in the second
145 panel of Figure 1. Note that the temperature decreases and the proton density increases
146 between the two current sheets. As in Figure 2, although Figure 3 can be explained by the
147 flux-tube-crossing scenario, it need not to be. The angles between δB and δV across the
148 two current sheets are 175 and 167 degrees. Unlike the first event, this double-current-sheet
149 is not associated with a reconnection exhaust. There was a slight but insignificant drop of
150 the magnetic field magnitude, so it is unlikely to be a magnetic hole. The proton number
151 density and proton temperature were also changed slightly at the two current sheets. These
152 slight changes, together with the pulse-like changes of the 3 magnetic field components,
153 suggest that this structure could be pulsed Alfvén wave (Gosling et al. 2011, 2012). Note,
154 if this was a pulsed Alfvén wave, then according to Figure 3(a) of Gosling et al. (2012)
155 and the fact that it has a duration of 46 seconds, it would be a long duration pulsed Alfvén
156 wave.

157 Figure 4 and Figure 5 show two triple-current-sheet events that occurred on 1995-10-2
158 and 1995-10-13, respectively. Consider first the event shown in Figure 4. Throughout the
159 event both B_y and V_y did not change much. B_x underwent a sharp change at 22:13:05 UT,

160 the first current sheet, after which it only changed slightly, until 22:25:00 UT when another
161 sharp change occurred and B_x returned to values similar to those before 22:13:00 UT. At
162 22:25:00 UT at the third current sheet another sharp change in B_x occurred. After the
163 crossing, B_x at and after 22:25:32 UT returned to a value comparable to B_x at 22:24:30
164 UT, just before crossing the 2nd current sheet. From the third panel, we can see that the
165 V_x changes at the same times as B_x .

166 Similar behavior also occurred to B_z and V_z . Before crossing the first current sheet
167 at 22:13:05 UT, B_z (V_z) was almost a constant. After the crossing, B_z increased and V_z
168 decreased. B_z also became slightly more turbulent. At the 2nd crossing at 22:25:00 UT, B_z
169 and V_z changed back to almost the same value as before 22:13:00 UT. Then both B_z and
170 V_z underwent another sudden change at the third current sheet crossing at 22:25:30 UT.
171 After the third crossing, B_z returned to a value similar to that before the 2nd crossing at
172 22:25:00 UT.

173 The magnitude of the magnetic field $|B|$ (the 2-nd panel), the proton number density
174 N_p and the proton temperature T_p (the 4-th panel) did not vary much throughout the
175 event. Before the crossing of the second current sheet, around 22:24:30 UT, $|B|$ increased
176 and N_p and T_p decreased. To better illustrate how the magnetic field direction evolves in
177 this event, we have constructed an animation of the evolution of the unit magnetic field \hat{B} .

178 Two facts worth to note: 1) various plasma properties, including N_p , T_p and the 3
179 components of \vec{B} and \vec{V} in the short period between 22:25:00 UT and 22:25:30 UT are very
180 similar to those prior to 22:13:00 UT, suggesting that these are the same solar wind plasma.
181 This can be clearly seen in the online animation. 2) similarly, the solar wind before and
182 after the short period are likely the same and it is different from that in 1).

183 One may attempt to explain this triple-current-sheet event as the spacecraft crossing
184 three uncorrelated individual current sheets that are generated by independent non-linear

185 interactions of the solar wind MHD turbulence. However, since independent current sheets
 186 have no correlations, the chance of the solar wind returning back to its original state after
 187 two independent current sheet crossings would be minute. Alternatively, one may argue
 188 that the plasma between 22:13:05 UT and 22:25:00 UT represented a rather long-lived
 189 transient structure, and interpret the first two current sheets as the boundaries of this
 190 structure. In such a case, one has to explain why after the third current sheet crossing,
 191 both the magnetic field and the plasma return to values the same as inside the transient
 192 structure.

193 Another triple-current-sheet event is the 1995-10-13 event, which is shown in Figure 5.
 194 Unlike the 1995-10-02 event, the 3-components of \vec{B} and \vec{V} , in particular, B_x and V_x ,
 195 suffered some additional changes at and around the three current sheets, making the
 196 1995-10-13 event less convincing than the 1995-10-02 event.

197 The first current sheet located at 19:32:28 UT. Both B_x and B_z showed a sudden jump
 198 across the first current sheet; V_x and V_z did not show significant changes. B_y and V_y also
 199 did not vary across the first current sheet. The current sheet is therefore non-Alfvénic.
 200 After crossing the first current sheet, B_z was almost a constant for the next ~ 7 minutes
 201 until 19:39:40 UT, where the second current sheet was encountered. It increased across the
 202 second current sheet to a value similar to those prior to the crossing of the first current
 203 sheet. Comparing to B_z , B_x was nearly constant after crossing the 1st current sheet for ~ 3
 204 minutes and then gradually increased until 19:39:00 UT, after which it increases noticeably
 205 before the second current sheet. Across the second current sheet, it dropped to a value
 206 similar to those prior to the crossing of the first current sheet. The third current sheet
 207 occurred at 19:40:15 UT. Across the third current sheet, there was a significant change
 208 of B_z and a small change of B_x . The two black horizontal dashed lines indicate that B_x
 209 (B_z) before the first current sheet was similar to B_x (B_z) between the second and the third

210 current sheets. The two magenta horizontal dashed lines indicate that B_x (B_z) between the
 211 first and the second current sheets was similar to B_x (B_z) after the third current sheet.
 212 Note that the change of B_x at the third current sheet was smaller than that at the second
 213 current sheet. After the third current sheet, B_x kept increasing, until 19:40:30 UT. The
 214 value of B_x after 19:40:30 UT is similar to those before 19:39:00 UT. As in the 1995-10-2
 215 event, we also constructed an animation of the evolution of the unit magnetic field \hat{B} for
 216 this event.

217 For the 1995-10-02 event, the angles between δB and δV across the three current sheets
 218 are 179° , 176° , and 174° , respectively. For the 1995-10-13 event, the angles between δB and
 219 δV are 155° , 124° and 173° , respectively. While the three current sheets in the 1995-10-02
 220 event are highly Alfvénic, those in the 1005-10-13 event are not.

221 3. Discussion and Summary

222 Current sheets are ubiquitous in the solar wind. They can be generated in-situ through
 223 non-linear interactions of the solar wind MHD turbulence (Greco et al. 2008, 2009), or
 224 represent the boundaries of flux tubes that originated at the Sun (Bruno et al. 2001;
 225 Borovsky 2008; Li et al. 2008). Appearing in pairs, they could also be the boundaries of
 226 reconnection exhausts ((Gosling 2011)).

227 An intriguing question one may ask is: for any particular current sheet, can we identify
 228 how it originated?

229 If current sheets that are generated in-situ and those that are convected out from
 230 the Sun have similar properties (such as the spread angles, the current sheet width, etc),
 231 then discriminating these two scenarios can be hard. However, as shown in the rightmost
 232 cartoon in Figure 1, the presence of triple-current-sheet event provides a strong support

233 to the flux-tube scenario. This is because in the flux-tube scenario the plasma and field
234 changes across the three current sheets are intimately correlated: as the spacecraft crosses
235 the three current sheets, the plasma before the first crossing and that between the 2nd and
236 the 3rd crossing are the same; the plasma between the first and the second crossings and
237 that after the third are the same. This is in stark contrast to the scenario where the current
238 sheets are generated in-situ. In the latter scenario, the plasma changes at the three current
239 sheets in a triple-current-sheet event need not match.

240 Note that the identification of a triple-current-sheet event does not tell us how many
241 single-current-sheet events are due to flux-tube crossing. As discussed earlier, since a
242 reconnection exhaust can be of large scale (Gosling 2007), some single-current-sheet events
243 we identify can be the boundaries of reconnection exhausts. Gosling (2010) identified an
244 occurrence rate of 40-80 reconnection events per month in solar minimum. In our study, we
245 only consider current sheets which are abrupt (width < 10 seconds) and whose spread angles
246 are larger than 45° , we find about 350 “single-current-sheet” events per month. Assuming
247 $2 * 60 = 120$ are boundaries of reconnection exhausts, then the rest are presumably either
248 generated in-situ or are the boundaries of flux tubes. Assuming 80% (50%) of the rest
249 are generated in-situ, then one gets about 45 (115) single-current-sheet events that are
250 flux-tube crossings per month.

251 If current sheets are boundaries of flux tubes that have a solar origin, e.g. super
252 granules, then one may expect to find some statistical correlations between in-situ
253 observations of current sheets and solar observation of super granules. Indeed, Bruno et al.
254 (2001) have suggested that the sizes of the flux tubes, when tracing back to the solar
255 surface, may correlate with the size of photospheric magnetic networks. In the work of
256 Miao et al. (2011), using Ulysses observation, the distribution of the waiting time statistics
257 of the current sheets were obtained. Assuming these flux tubes do not split or merge during

258 their propagation to 1 AU, then one may expect such waiting time statistics resembles the
259 distribution of the magnetic network sizes. Examining the waiting time statistics of current
260 sheet, and in particular, its dependence on heliocentric distance, and its correlation with
261 supergranule size will be reported in future work.

262 To conclude, we have examined 2-month’s worth solar wind data from the *Wind*
263 spacecraft and identified two triple-current-sheet events. The sequence of the observed
264 magnetic field and plasma data in these two events are in agreement with the scenario
265 where current sheets are flux tube boundaries, as depicted in Figure 1. Unambiguous
266 identification of flux tubes in the solar wind is important because these structures present
267 an additional source of solar wind MHD turbulence intermittency. They can affect the
268 power spectrum of the solar wind MHD turbulence (Li et al. 2011, 2012) as well as affecting
269 the transport of energetic particles in the solar wind (Qin and Li 2008).

270 We thank R.P. Lepping and R.P. Lin and the CDAWeb for making available the
271 data used in this paper and the referee for very valuable suggestions. This work is
272 supported in part by NSF grants ATM-0847719, AGS0962658, AGS1135432 and NASA
273 grant NNH07ZDA001N-HGI and NNX07AL52A.

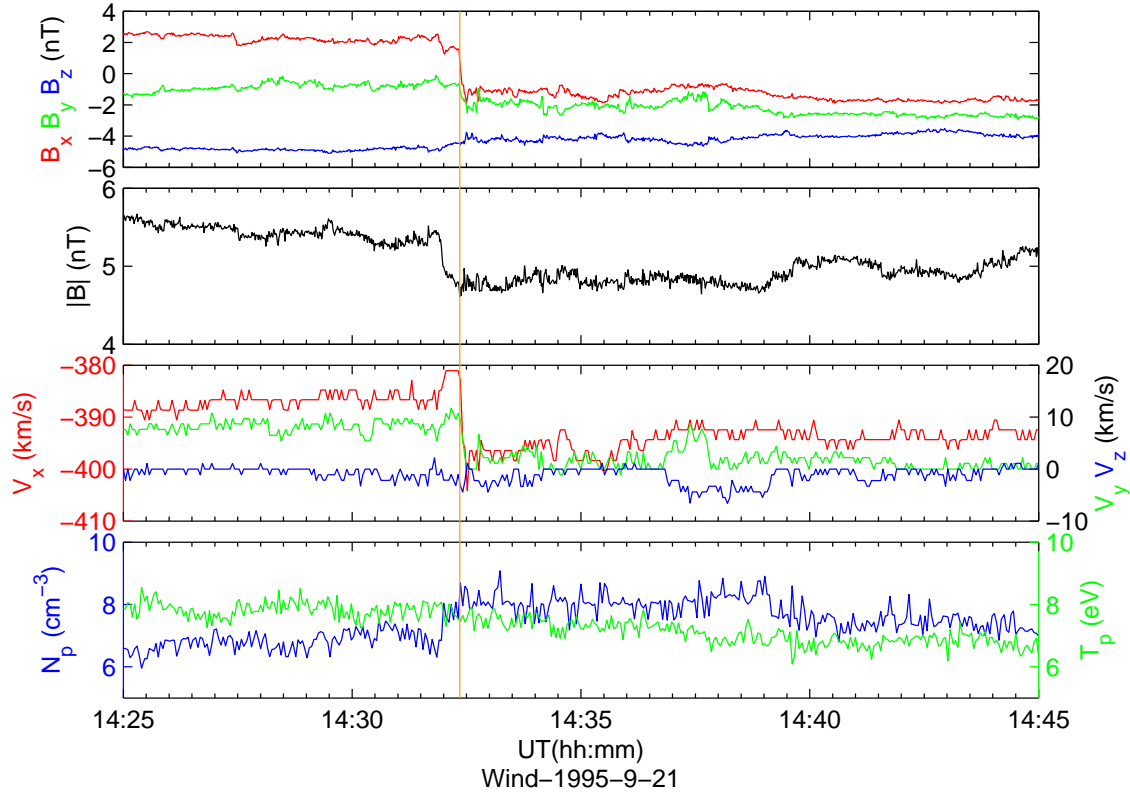


Fig. 2.— A single current sheet event occurred in 1995-09-21. Shown from top to bottom are the 3 components of the vector magnetic field in the Geocentric Solar Ecliptic (GSE) coordinate system, the magnitude of magnetic field, the 3 components of the vector proton velocity in the Geocentric Solar Ecliptic (GSE) coordinate system, and the solar wind proton number density and proton temperature, respectively. The brown vertical line marks the location of the current sheet.

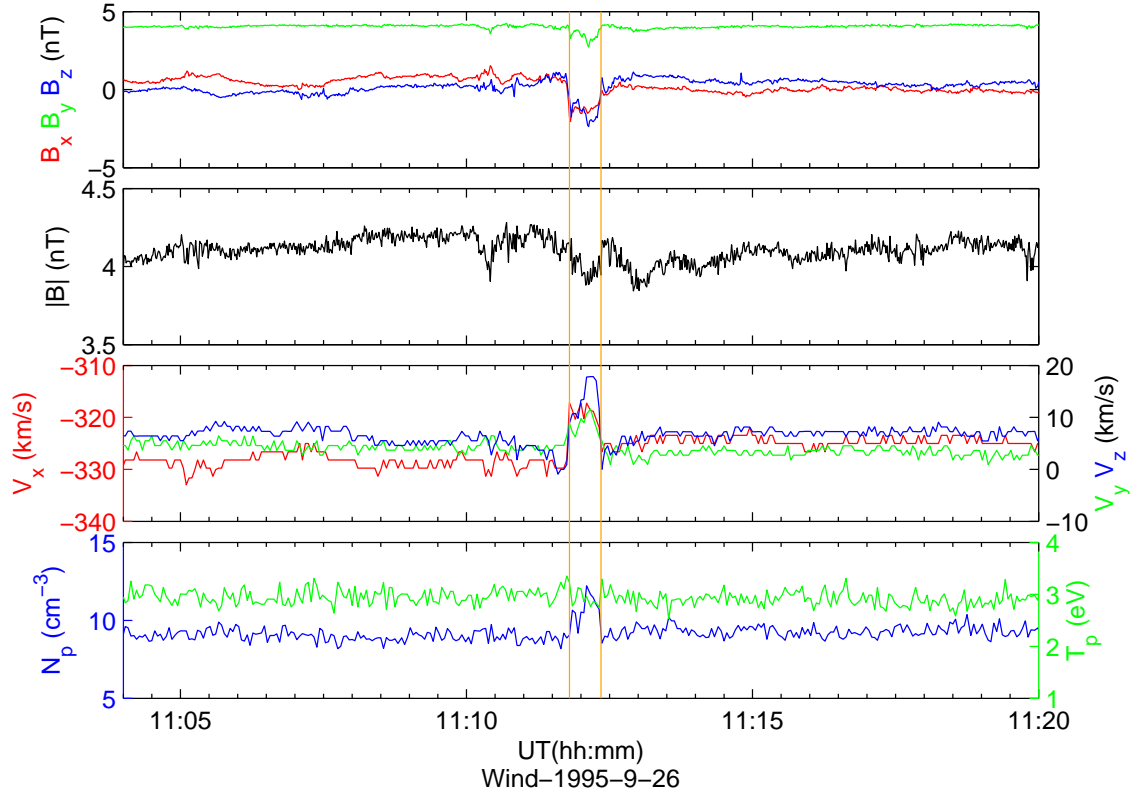


Fig. 3.— A double-current-sheet event that occurred in 1995-09-26. Shown from top to bottom are the 3 components of the vector magnetic field in the Geocentric Solar Ecliptic (GSE) coordinate system, the magnitude of magnetic field, the 3 components of the vector proton velocity in the Geocentric Solar Ecliptic (GSE) coordinate system, and the solar wind proton number density and proton temperature, respectively. The two brown vertical lines mark the location of the current sheet.

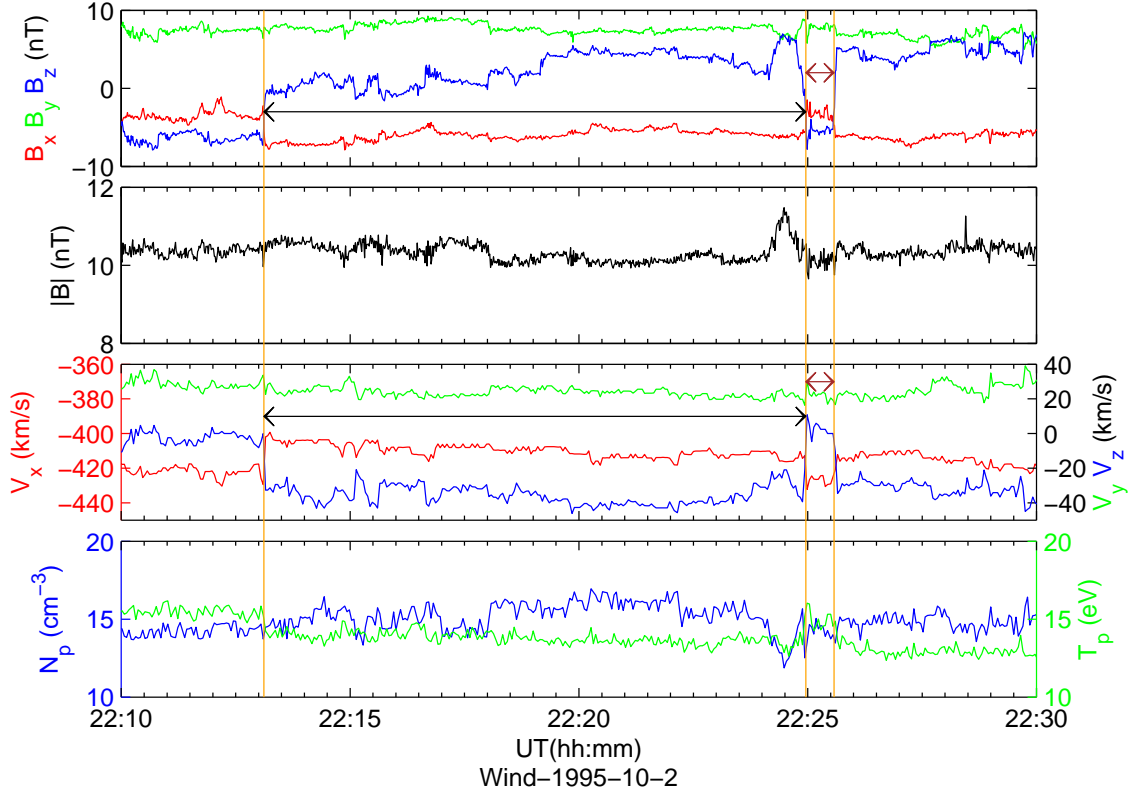


Fig. 4.— A triple-current-sheet event occurred on 1995-10-02. Shown from top to bottom are the 3 components of the vector magnetic field in the Geocentric Solar Ecliptic (GSE) coordinate system, the magnitude of magnetic field, the 3 components of the vector proton velocity in the Geocentric Solar Ecliptic (GSE) coordinate system, and the solar wind proton number density and proton temperature, respectively. The three vertical lines mark the location of the current sheet. Also see the online animation of the evolution of the unit magnetic field \hat{B} in this event.

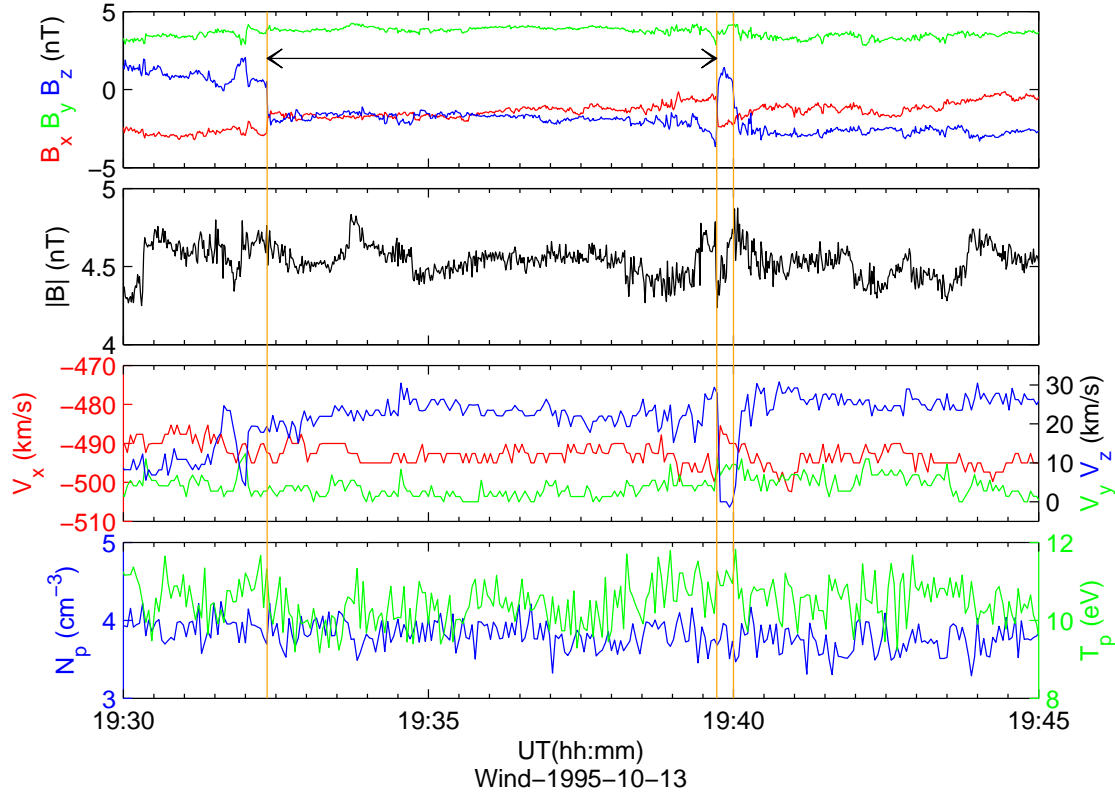


Fig. 5.— Same as Figure 4, but for the 1995-10-13 event. Shown from top to bottom are the 3 components of the vector magnetic field in the Geocentric Solar Ecliptic (GSE) coordinate system, the magnitude of magnetic field, the 3 components of the vector proton velocity in the Geocentric Solar Ecliptic (GSE) coordinate system, and the solar wind proton number density and proton temperature, respectively. The three vertical lines mark the location of the current sheet. Also see the online animation of the evolution of the unit magnetic field \hat{B} in this event.

REFERENCES

274

275 Boldyrev, S., 2006, Phys. Rev. Lett. 96, 115002

276 Boldyrev, S., Perez, J., 2009, Phys. Rev. Lett. 103, 225001

277 Iroshnikov, P. S., 1964, Soviet Astronomy, 7, 566-571

278 Kolmogorov, A., 1941, C. R. Acad. Sci. URSS, 30, 301-305

279 Kraichnan, R. H., 1965, Phys. Fluids, 8, 1385-1387

280 Borovsky, J. E., 2008, J. Geophys. Res-Space Phys., 113, A08110, doi:10.1029/2007JA012684

281 Borovsky, J. E., 2010, Phys. Rev. Lett. 105, 111102

282 Bruno, R., Carbone, V., Veltri, P., Pietropaolo, E., Bavassano, B., 2001, Planet Space Sci.

283 49 (12), 1201-1210

284 R. Bruno, R. D'Amicis, B. Bavassano, V. Carbone, and L. Sorriso-Valvo, 2007, Ann.

285 Geophys., 25, 19131927

286 Chang, T., Tam, S., Wu, C., APR 2004. Phys. Plasmas 11 (4), 1287–1299.

287 Greco, A., Matthaeus, W. H., Servidio, S., Chuychai, P. and Dmitruk, P., 2009, The

288 Astrophysical Journal Letters, 691, L111

289 Greco, A., P. Chuychai, W. H. Matthaeus, S. Servidio, and P. Dmitruk, 2008, Geophys.

290 Res. Lett., 35, L19111, doi:10.1029/2008GL035454

291 Gosling, J. T., Skoug R. M., McComas, D. J., Smith, C.W., 2005, JGR, 110, A01107.

292 Gosling, J. T., 2007, ApJL, 671, L73.

293 Gosling, J. T., 2010, 12th Solar Wind Conference, AIP 1216, 188.

- 294 Gosling, J. T., 2011, *Space Science Review*, 10.1007/s11214-011-9747-2
- 295 Gosling, J. T., Tian, H., and Phan, T. D., 2011, *ApJ*, 737, L35
- 296 Gosling, J. T., Tian, H., and Phan, T. D., 2012, *ApJ*, 751, L22
- 297 Lepping, R. L., et al., 1995, *Space Sci. Rev.*, 71, 207-229
- 298 Li, G., 2008, *Astrophys. J. Lett.* 672 (1), L65–L68
- 299 Li, G., Lee, E., Parks, G., 2008, *Ann. Geophys.*, 26, 1889–1895
- 300 Li, G., Miao, B., Hu, Q., Qin, G., 2011, *Phys. Rev. Lett.* 106, 125001
- 301 Li, G., Qin, G., 2011, Hu, Q., and Miao, B., 2012, *Adv. in Space Research*, 49, p1327-1332,
302 DOI: 10.1016/j.asr.2012.02.008
- 303 Lin, R. P., et al., 1995, *Space Sci. Rev.*, 71, 125-153
- 304 Miao, B., Peng, B., Li, G., 2011, *Annales Geophysicae* 29 (2), 237–249
- 305 Qin, G. and Li, G., 2008, *Astro. Phys. J.*, 682, L129-132. doi: 10.1086/591229
- 306 Ruzmaikin, A., Feynman, J., Goldstein, B., Smith, E., and Balogh, A., 1995, *J. Geophys.*
307 *Res-Space Phys.*, 100, 3395-3403
- 308 Tsurutani, B. T., and Smith, E. J., 1979, *J. Geophys. Res-Space Phys.*, 84, 27733
- 309 Tsurutani, B. T., G. S. Lakhina, O. P. Verkhoglyadova, E. Echer, F. L. Guarnieri,
310 Y. Narita, and D. O. Constantinescu, 2011, *J. Geophys. Res.*, 116, A02103,
311 doi:10.1029/2010JA015913.
- 312 Tu, C.-Y. and Marsch, E., 1991, *Ann. Geophys.*, 9, 319332

- ³¹³ Vasquez, B. J., V. I. Abramenko, D. K. Haggerty, and C. W. Smith, 2007, *J. Geophys. Res.*,
- ³¹⁴ 112, A11102, doi:10.1029/2007JA012504
- ³¹⁵ Zhou, Y., Matthaeus, W., Dmitruk, P., 2004, *Phys.* 76, 1015–1035